Green Chemical Engineering xxx (xxxx) xxx

Contents lists available at ScienceDirect

Green Chemical Engineering

journal homepage: www.keaipublishing.com/en/journals/green-chemical-engineering

Original Article

Machine learning aided investigation on the structure-performance correlation of MOF for membrane-based He/H_2 separation

Shitong Zhang [a,b], Yanjing He [a,c], Zhengqing Zhang [a,b,*], Chongli Zhong [a,b,**]

[a] State Key Laboratory of Separation Membranes and Membrane Processes, Tiangong University, Tianjin, 300387, China
[b] School of Chemical Engineering and Technology, Tiangong University, Tianjin, 300387, China
[c] School of Textile Science and Engineering, Tiangong University, Tianjin, 300387, China

HIGHLIGHTS

- The structure-performance relationship of MOFs for membrane based He/H_2 separation was investigated.
- PLD and ϕ were revealed as the most key features for determining membrane selectivity and He permeability, respectively.
- Pore surfaces terminated with highly electronegative atoms render membranes with improved membrane selectivity.

GRAPHICAL ABSTRACT

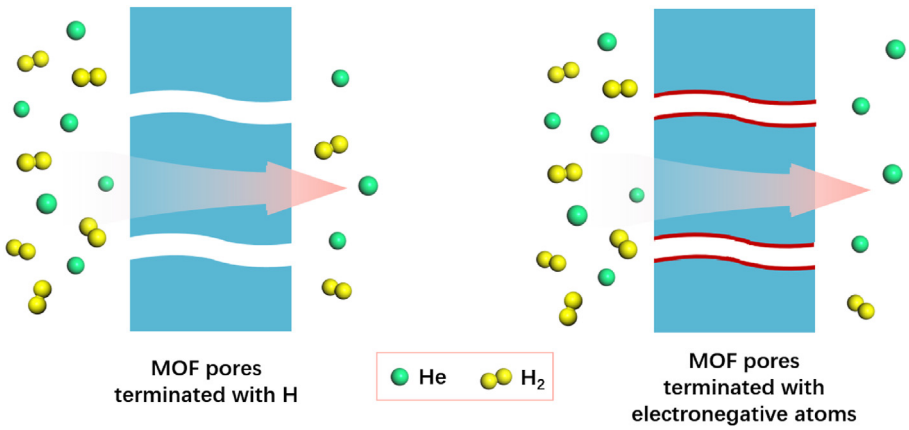

ARTICLE INFO

Keywords:
He/H_2
Membrane separation
Molecular simulation
Machine learning
DFT calculation

ABSTRACT

The separation of He/H_2 using membrane technology has gained significant interest in the field of He extraction from natural gas. One of the greatest challenges associated with this process is the extremely close kinetic diameters of the two gas molecules, resulting in low membrane selectivity. In this study, we investigated the structure-performance relationship of metal-organic framework (MOF) membranes for He/H_2 separation through molecular simulations and machine learning approaches. By conducting molecular simulations, we identified the potential MOF membranes with high separation performance from the Computation-Ready Experimental (CoRE) MOF database, and the diffusion-dominated mechanism was further elucidated. Moreover, random forest (RF)-based machine learning models were established to identify the crucial factors influencing the He/H_2 separation performance of MOF membranes. The pore limiting diameter (PLD) and void fraction (ϕ), are revealed as the most important physical features for determining the membrane selectivity and He permeability, respectively. Additionally, density functional theory (DFT) calculations were carried out to validate the molecular simulation results and suggested that the electronegative atoms on the pore surfaces can enhance the diffusion-based separation of He/H_2, which is critical for improving the membrane selectivities of He/H_2. This study offers useful insights for designing and developing novel MOF membranes for the separation of He/H_2 at the molecular level.

* Corresponding author. State Key Laboratory of Separation Membranes and Membrane Processes, Tiangong University, Tianjin, 300387, China.
** Corresponding author. State Key Laboratory of Separation Membranes and Membrane Processes, Tiangong University, Tianjin, 300387, China.
E-mail addresses: zhangzhengqing@tiangong.edu.cn (Z. Zhang), zhongchongli@tiangong.edu.cn (C. Zhong).

https://doi.org/10.1016/j.gce.2024.01.005
Received 21 September 2023; Received in revised form 30 January 2024; Accepted 31 January 2024
Available online xxxx

Please cite this article as: S. Zhang et al., Machine learning aided investigation on the structure-performance correlation of MOF for membrane-based He/H_2 separation, Green Chemical Engineering, https://doi.org/10.1016/j.gce.2024.01.005

1. Introduction

Helium (He) is widely applied in biomedical science, nuclear facilities, and space industries, owing to its chemical inertia, ultralow boiling point (−4.15 K), and intrinsic lightness in mass [1–3]. Up to now, the extraction of He from natural gas is still the only industrialized way to obtain high-purity He resources [2], which is mainly achieved by combining cryogenic distillation methods and subsequent pressure swing adsorption techniques [4]. However, this process is quite energy-intensive [5], and in addition, the great demand for He and its limited production has further led to a global He shortage and a sharp price increase over the past few years [2], which has aroused growing interest towards more efficient and cost-friendly He purification methods.

Among the various strategies, membrane-based gas separation is regarded as very promising in tackling energy and environmental challenges, which takes versatile advantages in terms of less energy consumption, more environment-friendly manufacturing, and process simplicity when compared with traditional gas separation technologies [2,4,6]. As a result, considerable efforts have been devoted to membrane-based He separation [5–8]. Currently, various separation membranes have been fabricated for He extraction and they usually show superior performance in the separation of He/CH_4 [2,9,10] and He/N_2 [11,12], due to the significantly smaller kinetic diameter of He compared with that of CH_4 and N_2 (2.60 Å for He, 3.80 Å for CH_4, and 3.64 Å for N_2) [4,13,14]. However, for the membrane separation of He from H_2 (another common component of natural gas), the extremely similar kinetic diameters between them (2.90 Å for H_2) pose a great challenge to the fabrication of corresponding separation membranes, which usually display relatively low separation selectivities below ~5 according to published reports [2,9,15,16]. From this view of point, it is still of crucial importance to unravel the underlying structure-performance correlation to provide guidelines for the design of novel separation membranes with high He/H_2 separation performance.

In recent years, metal-organic frameworks (MOF) have experienced rapid development as an emerging class of porous material, and their highly regulable pore structures and pore surface chemistry make them quite attractive to be fabricated into separation membranes [17,18]. As reported, when being applied for gas separations, many MOF-based membranes are able to exceed the Robeson upper bounds for multiple gas pairs [2,19], even including typical difficult separation systems (*e.g.*, CH_4/N_2 [20,21], CO_2/CH_4 [22,23], and CO_2/N_2 [24,25]). However, it is not easy to rapidly identify the MOFs from the vast database for fabricating membranes with high He/H_2 separation performance. Specifically, to date, the separation factors for the mixture of H_2 and He are generally as low as less than 3, according to the experimental studies using MOF-based membranes [26–29]. There are also extensive high throughput computational screening-based studies on the membrane separation of He [4,30,31], which however often adopted MOF structures with pore limiting diameter (PLD) values at least higher than 3.64 Å, considerably larger than the kinetic diameters of He and H_2. Therefore, the related results could not fully reflect the separation potentials of MOF membranes for He/H_2 pair, given that too large pores of membranes tend to generate low selectivity because of the reduced effects of gas-pore interactions on the separation performance. In present study, we comprehensively evaluated the theoretical performance of Computation-Ready, Experimental MOFs (CoRE MOFs) [32] for He/H_2 membrane separation, accordingly identified the most promising candidates and revealed the gas separation mechanism. In addition, machine learning (ML) approach was further applied to establish the structure-performance correlation of MOF membranes for He/H_2 selectivity and He permeability. Density functional theory (DFT) computations were also performed and illustrated that the mechanism of the diffusion separation can be regulated by the surfaces of MOF pores terminated with highly electronegative atoms.

2. Computational details

2.1. MOF database

The CoRE MOFs were employed to study the performance of MOF-based membrane separation for He/H_2 mixture. The structural characteristics of these MOFs, including void fraction (ϕ), PLD, largest cavity diameter (LCD), accessible volume (AV), density (ρ), and free volume (V_{free}), were calculated using Zeo++ program [33]. A spherical radius of 1.82 Å was used to mimic N_2 as a probe molecule. The MOF structures with zero AV and V_{free} values were not considered in the subsequent screening, and additionally we only employed the structures with PLDs > 2.90 Å to ensure that both He and H_2 were able to translate through the membrane pores. Finally, 7877 MOFs were preserved for further screening explorations, including molecular simulation and machine learning studies.

2.2. Molecular simulations and DFT calculations

The adsorption of a He/H_2 (50/50) mixture was simulated using Grand Canonical Monte Carlo (GCMC) at 298.0 K and 1.0 bar. All atoms of MOFs were fixed and the non-bonded force field parameters were described using the Universal Force Field (UFF) [34]. Besides, the atomic point charges of MOFs were assigned using the extended charge equilibration (EQeq) method [35]. Although utilizing charges calculated at the DFT level can more accurately reflect the charge distribution in MOF membranes, and a few ML models that can predict the values of these charges have already been published [36], the EQeq method remained sufficiently accurate for this study on the structure-performance relationships of MOFs, considering its reliability has been validated by extensive simulation studies on MOF-based materials [37,38]. The potential parameters of H_2 and He were derived from published studies [31,39,40], as displayed in Table S1. The total Monte Carlo cycles for each GCMC simulation were set to 3×10^7, and the data from the final 2×10^7 cycles was employed for calculating the adsorption properties. Accordingly, the adsorbed amount of He (H_2) in each MOF was computed and adopted for calculating the diffusivities of the gas molecules using equilibrium molecular dynamics (EMD) simulations in the canonical (NVT) ensemble at 298.0 K. A time step of 1.0 fs was applied to the velocity Verlet algorithm to integrate the equations of motion. We ran three independent EMD simulations of 10.0 ns for each MOF structure and the data from the last 3.0 ns was collected for assessing the diffusion of He and H_2. The Ewald sum method was employed to handle the long-range electrostatic interactions, and we adopted the Lorentz-Berthelot (LB) mixing method to treat all the cross-interactions between different particles. The distance cutoff was set to 1.2 nm for calculating both Lennard-Jones (LJ) and Coulomb interactions. Besides, the periodic boundary conditions (PBC) were applied in all directions. All these force field-based simulations (GCMC and EMD) were carried out using our in-house HT-CADSS suite [41]. On the basis of the GCMC and EMD results, the separation performances of MOF membranes were deduced according to our previous report [42]. Based on such computation strategy, we compared the computational He (H_2) permeance and membrane selectivity with the experimental results, and demonstrated a total agreement between them, as shown in Fig. S1 and Table S2. Notably, the calculated H_2 permeability of Cu-BTC membranes in this study (8.5×10^4 Barrer) was lower than that in Daglar et al.'s [30] study (~2.0×10^5 Barrer), but also in agreement with the experimentally measured values (5.8×10^4–2.7×10^5 Barrer) [43,44]. These results validated the present simulation method for evaluating the gas permeability and membrane selectivity of the MOF membranes.

DFT calculations were also performed within the CASTEP program [45] to further investigate the diffusion mechanism of He (H_2) in 6 representative MOFs. The exchange-correlation potential was described by the Perdew-Burke-Ernzerhof (PBE) generalized gradient approach

(GGA) [46,47]. The Tkatchenko-Scheffler method [48] was applied for the calculations of DFT dispersion correction. Brillouin zone sampling was exerted using a 2 × 2 × 2 *k*-point mesh. Ultrasoft pseudopotentials was also employed in this study. Self-consistent field (SCF) converged criterion was set to 1.5×10^{-6} eV/atom and converge criterion of structure optimization was 1.0×10^{-5} eV/atom. During the geometry optimizations, the Kohn-Sham orbitals were computed using a plane-wave basis set with a cutoff energy of 330.0 eV. The single point calculation was further performed with a SCF tolerance of 1.0×10^{-6} eV/atom and a plane-wave kinetic energy cutoff of 400.0 eV.

2.3. Machine learning (ML)

We collected the results of molecular simulations, along with physical and chemical descriptors for training and testing the ML model. Specifically, the random forest (RF) algorithm was used to establish ML models because of its superior performance in predicting the separation of diverse MOFs for different gas pairs [49,50]. The ML studies was implemented using the scikit-learn module [51] in Python and the crucial factors that affecting the separation performance can be revealed with the established RF model. Various physical and chemical descriptors were extracted from the MOF database by Zeo++ calculations and our in-house code, such as the unit volume (V), ρ, LCD, PLD, AV, V_{free}, ϕ, maximum (q_1) and minimum (q_2) of the partial charge of atoms, content of O, N, S and halogen elements, metals, and diverse linkers. To improve the performance of ML studies and avoid overfitting, the representative descriptors were first collected, among which the ones with strong correlation (the Pearson correlation coefficient $>$ 0.9) were further removed, as shown in Fig. S2. At last, 6 structural features (ρ, V_{free}, AV, LCD, PLD, and ϕ), two charge descriptors (q_1 and q_2), and all the other chemical descriptors were adopted for establishing the ML models. Subsequently, we randomly collected 80% of the simulation results to the training set and the rest (20%) to the test set. The final accuracy of the model was assessed by the determination coefficient (R^2) and root mean square error (RMSE).

3. Results and discussion

3.1. Computational screening of high-performance MOF membranes

To investigate the correlation between the structure and performance of MOF membranes for He/H_2 separation, we initially conducted a high throughput theoretical screening of MOF membranes using a binary mixture of He/H_2 at 298 K and 1.0 bar. Fig. 1 illustrates the simulated He permeabilities and He/H_2 selectivities of the selected membranes. Our findings reveal that a significant number of the structures from the MOF database exhibit membrane selectivity to He and surpass the latest 2019 upper bound [15]. However, the permeability-selectivity trade-off effect remains a major limitation in improving the separation performance of MOF membranes for He/H_2 separation. For instance, the structure named ILUGAY demonstrates the highest membrane selectivity (70.0), but its corresponding He permeability (2341 Barrer) is relatively lower compared with other MOFs. In order to quantitatively assess the overall membrane performance, the membrane performance score (MPS) was employed, which was defined and validated in our previous studies on gas mixture separations using membranes [42,52]. Consequently, we selected the top 10 MOF membranes with the greatest MPS values and significant membrane selectivity ($>$ 3.0) as the most promising candidates for He/H_2 separation (Fig. S3 and Table S3).

To reveal the mechanism underlying the membrane separation process, we further analyzed the adsorption and diffusion selectivities of MOF membranes for the separation of He/H_2. As shown in Fig. S4, more than half of the MOF structures exhibit selective adsorption of H_2 over He, as the latter is chemically inert and less prone to adsorption. In the case of diffusion selectivity, He displays higher diffusion rate than H_2 in about half of the MOF membranes (Fig. S4), and there exists a

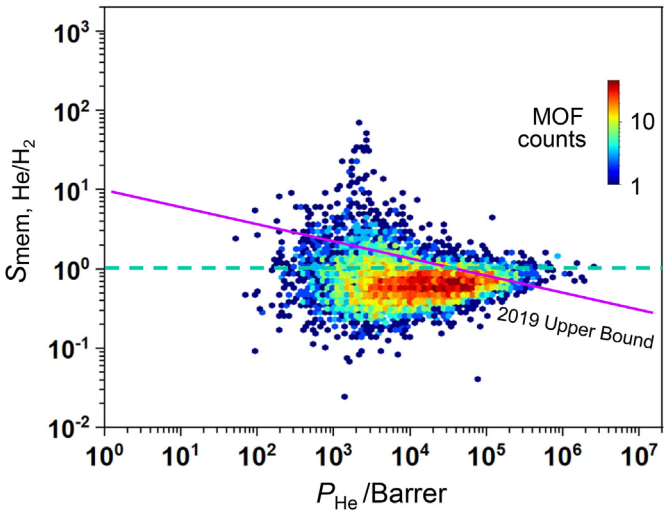

Fig. 1. Relationship between He permeability and membrane selectivity of MOF membranes for the separation of He/H_2.

significantly positive correlation between membrane selectivity and diffusion selectivity (Fig. 2). These findings demonstrate that the membrane process is dominated by the differential diffusivities of gas molecules. This indicates that improving the membrane separation selectivity for He purification by regulating the diffusion behaviors in the membrane pores is more effective compared to modifying the adsorption effect.

3.2. Disclose the relative importance of MOF features

RF-based ML models were established to investigate the key factors affecting the He/H_2 membrane selectivity and He permeability. As shown in Fig. 3a, the data points of the prediction of membrane selectivity are distributed around upward inclined straight lines and concentrated on the diagonal, corresponding to an R^2 of 0.78 and an RMSE of 0.77. This indicates an overall good prediction of the membrane selectivity values. To confirm the stability of the RF model, the prediction was repeated four more times, and the results showed negligible variations (Fig. S5), suggesting that the established RF algorithm is effective for uncovering the hidden relationship between MOF features and their membrane selectivities. The relative importance of MOF structural

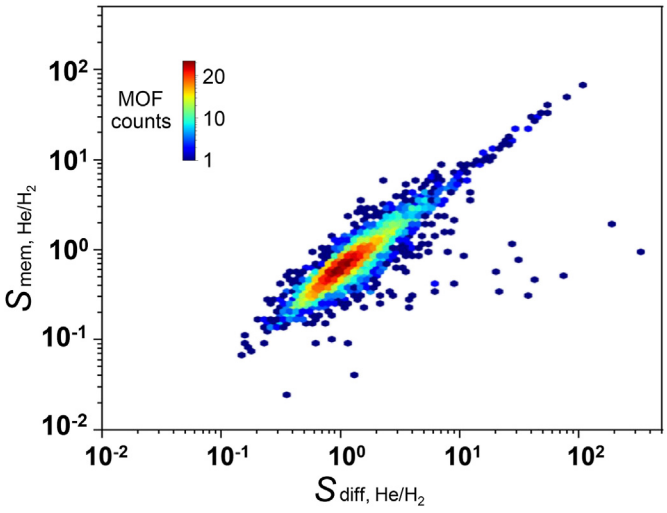

Fig. 2. Relationship between membrane and diffusion selectivity of MOF membranes for the separation of He/H_2.

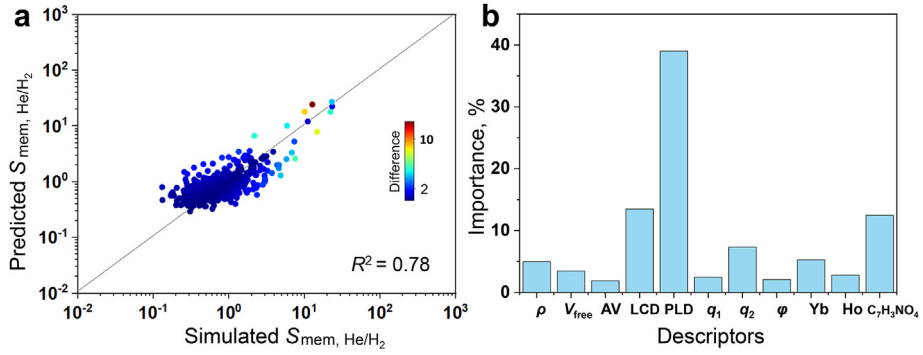

Fig. 3. (a) Predicted He/H_2 selectivity of MOF membranes *via* ML model of RF against the simulated results from molecular simulations; (b) relative importance of various MOF features suggested *via* RF model for predicting the membrane selectivity of He/H_2.

features was thus revealed according to the established RF model. As shown in Fig. 3b, PLD is the most critical factor determining the membrane selectivity (39.0%) among the MOF physical descriptors. The relative importance of the other descriptors was ranked in the following order: LCD (13.49%) > $C_7H_3NO_4$ (12.46%) > q_2 (7.30%) > Yb (5.25%) > ρ (4.96%). The findings could supply guidance for the design and fabrication of novel MOF membranes with excellent He/H_2 separation factors.

Furthermore, the RF algorithm-based ML model also displayed good accuracy for predicting He permeability with a high R^2 value (0.87) (Fig. 4). The results of four other repeated predictions of He permeability using the RF model are shown in Fig. S6, also displaying minor variations. The structural feature ϕ plays the most important role in governing He permeability (58.88%), in line with the result from Daglar et al.'s [30] report. In addition, the other relatively important descriptors include PLD (13.22%) > ρ (6.65%) > AV (4.56%) > content of O, N, S, and halogen elements (2.60%) for He permeability. It can be found that the He permeability is mainly influenced by the structural features of MOFs, and chemical features of MOF only display minor effects owing to the chemical inertness of He.

3.3. Structure-performance correlations

Based on the screening data, further understanding of the structure-performance correlation can guide the design and fabrication of novel MOF membranes for effective He/H_2 separation. In this study, we analyzed the effects of four features on the He/H_2 selectivity of MOF membranes (Fig. 5). As shown in Fig. 5a, with increased PLD, the He selectivity of MOF membranes decreased rapidly. Specifically, when the PLD value is larger than 3.30 Å, the He selectivity in each bin of the histogram becomes lower than 1, indicating that MOF membranes with large PLD values tend to show higher H_2 selectivities (Fig. 5a). The relationship between LCD and He/H_2 membrane selectivities is displayed in Fig. 5b. It can be observed that MOF membranes with relatively small LCD (3.10–4.10 Å) also exhibit He selectivity. Moreover, numerous MOFs with LCD values ranging from 7.10 to 8.10 Å and 11.10–12.10 Å have PLD values smaller than 3.30 Å, and display pronounced He selectivity (Fig. S7).

It is noteworthy that the model of the H_2 molecule used in molecular simulations comprises two hydrogen atoms and a dummy site (H_COM) located at the molecular center of mass. Partial charges are assigned to the hydrogen atoms and the dummy atom (Table S1) with the aim of reproducing the quadrupole moment of the hydrogen molecule; while the model of He only contains a zero-charged atom. Consequently, we introduce charge descriptors (*i.e.*, q_1 and q_2) to examine their impact on separation performance. The established RF model for predicting He/H_2 membrane selectivity (Fig. 3b) indicates that the value of q_2 (the most negative charge in each MOF structure) has a more significant influence than q_1 (the most positive charge in each MOF structure). Therefore, we further analyzed the relationships between q_2 and the selectivity. As displayed in Fig. 5c, the membrane selectivity of He slightly increases with the increasing value of q_2, and the optimal q_2 is in the range of −0.88 and −0.58 e. We further found that when the values of q_2 in MOFs are less negative, the adsorptive selectivity of He becomes relatively higher (Fig. S8), leading to increased membrane selectivities of He.

Moreover, the higher relative importance of q_2 (Fig. 3b) suggests that the negatively charged sites are more effective in generating distinct gas-MOF interactions for H_2 and He. Thus, we also examined the relationship between the content of O/N/S/halogen elements (which are typically negatively charged in simulation models) and He membrane selectivities. As illustrated in Fig. 5d, when the content of these highly electronegative atoms is below 80 mol/mol, it has negligible effects on the membrane selectivity of He. However, when the content exceeds 80 mol/mol, the associated MOF membranes exhibit significantly increased He

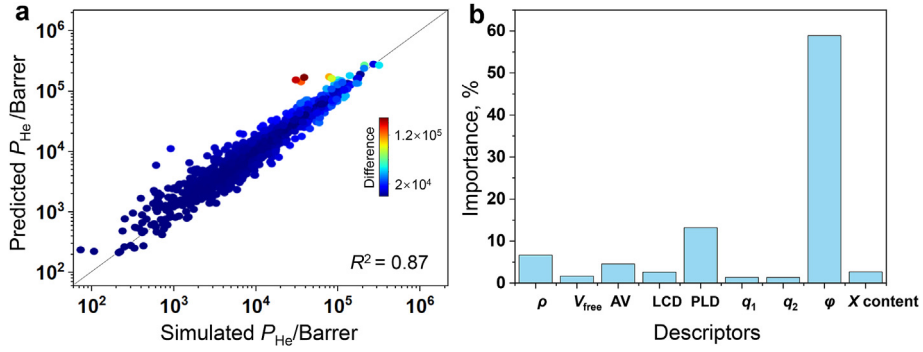

Fig. 4. (a) Predicted He permeability of MOF membranes *via* ML model of RF against the simulated results from molecular simulations; (b) relative importance of different MOF features revealed *via* RF model for predicting the He permeability of MOF membranes. *X* content means the content of O, N, S, and halogen (the unit is mol/mol).

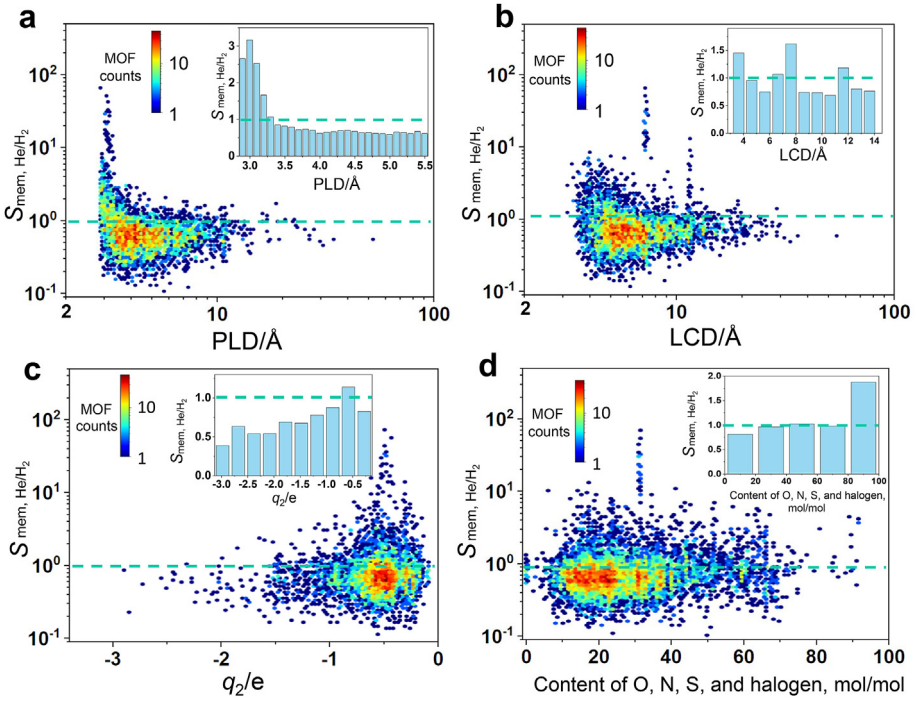

Fig. 5. Structure-performance relationships of MOF membranes for He/H_2 selectivity. The plotted are membrane selectivities of He over H_2 as functions of (a) PLD, (b) LCD, (c) q_2, and (d) content of O, N, S, and halogen atoms. The inset histogram in each panel displays the average He/H_2 membrane selectivity associated with varying values of descriptors.

selectivity, mainly due to the substantial increase in diffusion selectivity (Fig. S9). Since the gas-MOF interactions to regulate the diffusion separation of He/H_2 mainly occur in the pores, we proposed that the negatively charged atoms on the pore surfaces might be able to modulate the membrane selectivity of He/H_2 (see more below in Section 3.4).

For the He permeability of MOF membranes, we mainly investigated the influence of ϕ and PLD. As illustrated in Fig. 6, it is evident that with the increase of ϕ and PLD (in the range of 0–30 Å), the permeability of MOF membranes for He also significantly increases. This result can be explained by the fact that larger pore sizes typically impose less resistance to the diffusion of gas molecules, and a higher number of through pores within the membrane per unit area (which directly corresponds to a higher value of ϕ) can simultaneously lead to increased gas permeation. Considering that large PLD values are generally detrimental to membrane selectivity of gas separation in pores and ϕ has little effect on the membrane selectivity of He/H_2 (Fig. 3b), this result suggests that it is an optimal method to enhance the He permeability by increasing the ϕ of MOFs when designing novel membranes for the separation of He/H_2.

3.4. DFT studies on the diffusion mechanisms

To further understand the effect of highly electronegative atoms on the diffusion selectivity of He/H_2, we performed DFT calculations to study the diffusion mechanisms of He and H_2 translocating through six representative MOF pores, including three MOF pores with abundant O, N, and Cl atoms (from XALTOV, WEYQAU16, and BOCTEU01) and three pore structures mainly composed of C and H atoms (from MECWEX, MAGVOG22, and LETVUB). Additionally, the six MOF structures were selected based on their PLD values being around 3.0 Å to reduce the interference of pore sizes on the comparison between the two groups. As shown in Fig. S10, the calculated gas-MOF interaction energies using DFT were compared with those from the simulations based on UFF method, both of which indicated relatively stronger binding affinity of H_2 in MOFs than that of He. The discrepancy between the two methods was comparable to that found in the study of Smit and co-workers [53].

Representative results of the DFT calculations using XALTOV and MECWEX were displayed in Fig. 7. When gas molecules mitigate through

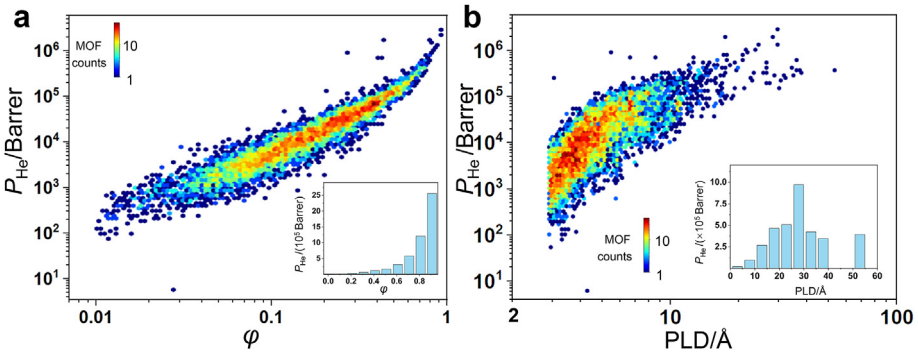

Fig. 6. Structure-performance relationships of MOF membranes for He permeability. Plotted are He permeabilities as functions of (a) ϕ and (b) PLD. The inset histogram in each panel displays the average He permeability associated with varying values of ϕ or PLD.

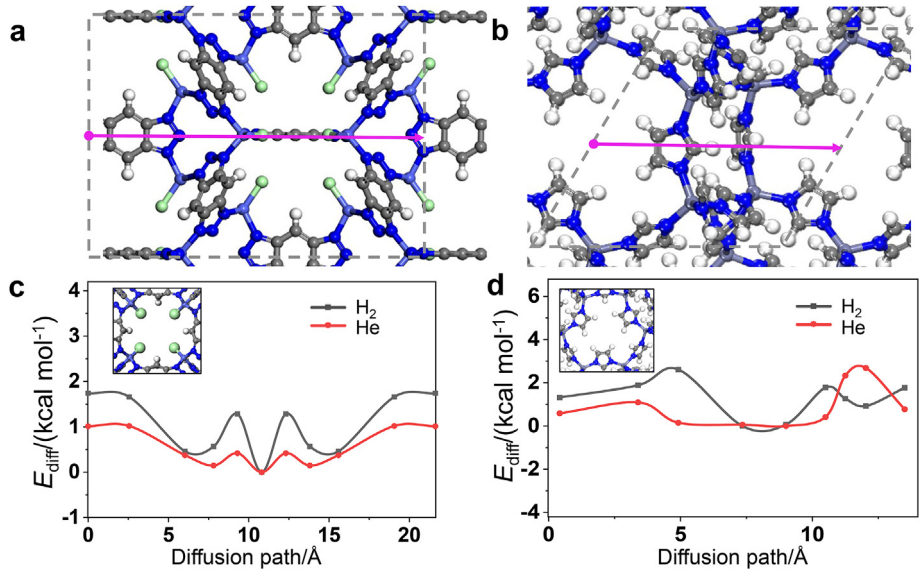

Fig. 7. The diffusion routes of gas molecules in the pores of (a) XALTOV and (b) MECWEX; the energy profiles along the diffusion path of H_2 (black lines) and He (red lines) in the pores of (c) XALTOV and (d) MECWEX. The insets in (c) and (d) display the top views of the corresponding pores (color code: white, H; blue, N, gray, C; light green, Cl; light blue, Co; slate-gray, Zn).

the MOF (XALTOV) pore with terminated Cl atoms (Fig. 7a), the minima of the resulting energy profiles are located at the center of the diffusion path, which are surrounded by four Cl atoms and correspond to the most favorable adsorption sites for H_2 and He molecules (Fig. 7c). Importantly, the diffusion barrier (1.73 kcal mol^{-1}) for H_2 migrating from the most stable adsorption site to the neighboring unit cell is relatively higher than that for the migration of He (1.01 kcal mol^{-1}), indicating a more rapid diffusion of He molecules through the membranes. In contrast, according to the energy profiles of gas migration through pore structures composed of terminated H atoms in MECWEX (Fig. 7b), the energy barriers for the diffusion of the two gas molecules are very close to each other (Fig. 7d), thus leading to negligible diffusion selectivity of He/H_2. Similar results were also obtained in the cases of the other four structures: the surface migration of H_2 in pore structures terminated with highly electronegative atoms shows relatively higher diffusion barriers (Fig. S11) than that of He; meanwhile the diffusion barriers of H_2 and He are much more comparable in the pores terminated with H atoms (Fig. S12). Besides, the GCMC and EMD results suggested that both the diffusion and membrane selectivities of He/H_2 using XALTOV, WEYQAU16, and BOCTEU01 membranes are significantly higher than those using MECWEX, MAGVOG22, and LETVUB membranes (Table S4). These findings indicate that modifying the pore surfaces with highly electronegative elements can facilitate the separation of He/H_2 *via* the diffusion process.

4. Conclusions

In this work, we combined molecular simulations and ML studies to investigate MOF for membranes-based He/H_2 separation. Based on molecular simulation studies, we identified the top 10 performing MOF membranes as the most promising candidates for separating He/H_2 binary mixtures, exhibiting both high He permeability and membrane selectivity. Furthermore, we found that the gas membrane separation process is predominantly governed by diffusion for most MOF membranes. ML studies revealed the relative importance of various physical and chemical descriptors influencing He/H_2 selectivity and He permeability, based on an accurate RF model ($R^2 \geq 0.78$). Our findings indicate that PLD and ϕ display the most critical effects on the membrane selectivity of He/H_2 and He permeability, respectively. Further analysis of the structure-performance relationship suggested that MOFs with optimal PLD (2.90–3.30 Å), LCD (3.10–4.10 Å), and $C_7H_3NO_4$ linkers can result in relatively high membrane selectivity. Additionally, we unraveled that electrostatic interactions can regulate the diffusion selectivity of He/H_2, as the H_2 model exhibits polarized electrostatic potential. DFT calculations further confirmed that pore surfaces terminated with electronegative atoms can promote the diffusion separation of He/H_2. This work may provide helpful insights for the development of novel MOF membranes for highly efficient separation of He/H_2.

CRediT authorship contribution statement

Shitong Zhang: Writing – original draft, Supervision, Methodology, Investigation. **Yanjing He:** Investigation. **Zhengqing Zhang:** Writing – review & editing, Supervision, Investigation, Funding acquisition. **Chongli Zhong:** Supervision.

Declaration of competing interests

The authors declare that they have no known competing financial interests or personal relationships that could have appeared to influence the work reported in this paper.

Acknowledgments

This work is supported by the National Natural Science Foundation of China (Nos. 22141001 and 22108202).

Appendix A. Supplementary data

Supplementary data to this article can be found online at https://doi.org/10.1016/j.gce.2024.01.005. Comparison of molecular simulations of gas permeability with the published experimental results (Fig. S1); matrix of Pearson correlations between the descriptors (Fig. S2); the models of the top 10 performing MOFs (Fig. S3); relationship between adsorption and diffusion selectivity of MOF membranes for the separation of He/H_2 (Fig. S4); four repeated predictions of He/H_2 selectivity of MOF membranes using RF model (Fig. S5); four repeated predictions of He permeability of MOF membranes using RF model (Fig. S6); relationship among membrane selectivity of He/H_2, LCD and PLD of MOFs (Fig. S7); relationship between q_2 and adsorption selectivity of MOF membranes for the separation of He/H_2 (Fig. S8); effects of the content of

highly electronegative atoms on the adsorption and diffusion selectivities (Fig. S9); comparison of the gas-MOF interaction energies from DFT and force field methods (Fig. S10); the diffusion routes and related energy profiles of gas molecules translocating in the pores of BOCTEU01 and WEYQAU16 (Fig. S11); the diffusion routes and related energy profiles of gas molecules translocating in the pores of LETVUB and MAGVOG22 (Fig. S12); potential parameters for the models of He and H_2 (Table S1); comparison of membrane selectivity between the computational and experimental results (Table S2); top 10 performing MOF for membrane-based He/H_2 separation (Table S3); simulated performance of 6 representative MOF membranes (Table S4).

References

[1] T.E. Rufford, K.I. Chan, S.H. Huang, E.F. May, A review of conventional and emerging process technologies for the recovery of helium from natural gas, Adsorpt. Sci. Technol. 32 (2014) 49–72.
[2] Z. Dai, J. Deng, X. He, C.A. Scholes, X. Jiang, B. Wang, H. Guo, Y. Ma, L. Deng, Helium separation using membrane technology: recent advances and perspectives, Sep. Purif. Technol. 274 (2021) 119044.
[3] P. Haussinger, R. Glathaar, W. Rhode, H. Kick, C. Benkmann, J. Weber, H.J. Wunschel, V. Stenke, E. Leicht, H. Stenger, Noble gases, in: F. Ullmann (Ed.), Ullmann's Encyclopedia of Industrial Chemistry, John Wiley and Sons Inc., New Jersey, 2011, pp. 392–448.
[4] O. Kadioglu, S. Keskin, Efficient separation of helium from methane using MOF membranes, Sep. Purif. Technol. 191 (2018) 192–199.
[5] C.A. Scholes, G.W. Stevens, S.E. Kentish, Membrane gas separation applications in natural gas processing, Fuel 96 (2012) 15–28.
[6] Y. Wang, J. Li, Q. Yang, C. Zhong, Two-dimensional covalent triazine framework membrane for helium separation and hydrogen purification, ACS Appl. Mater. Interfaces 8 (2016) 8694–8701.
[7] A. Soleimany, S.S. Hosseini, F. Gallucci, Recent progress in developments of membrane materials and modification techniques for high performance helium separation and recovery: a review, Chem. Eng. Process 122 (2017) 296–318.
[8] J. Schrier, Helium separation using porous graphene membranes, J. Phys. Chem. Lett. 1 (2010) 2284–2287.
[9] M. Yavari, M. Fang, H. Nguyen, T.C. Merkel, H. Lin, Y. Okamoto, Dioxolane-based perfluoropolymers with superior membrane gas separation properties, Macromolecules 51 (2018) 2489–2497.
[10] C. Chen, A. Ozcan, A.O. Yazaydin, B.P. Ladewig, Gas permeation through single-crystal ZIF-8 membranes, J. Membr. Sci. 575 (2019) 209–216.
[11] A. Labropoulos, G. Romanos, N. Kakizis, G. Pilatos, E. Favvas, N. Kanellopoulos, Investigating the evolution of N_2 transport mechanism during the cyclic CVD post-treatment of silica membranes, Microporous Mesoporous Mater. 110 (2008) 11–24.
[12] C.A. Scholes, U. Ghosh, Helium separation through polymeric membranes: selectivity targets, J. Membr. Sci. 520 (2016) 221–230.
[13] C. Gong, X. Peng, M. Zhu, T. Zhou, L. You, S. Ren, X. Wang, X. Gu, Synthesis and performance of STT zeolite membranes for He/N_2 and He/CH_4 separation, Sep. Purif. Technol. 301 (2022) 121927.
[14] H. Molavi, A. Shojaei, S.A. Mousavi, Improving mixed-matrix membrane performance *via* PMMA grafting from functionalized NH_2–UiO-66, J. Mater. Chem. A 6 (2018) 2775–2791.
[15] A.X. Wu, J.A. Drayton, Z.P. Smith, The perfluoropolymer upper bound, AlChE J 65 (2019) e16700.
[16] T. Van Gestel, J. Barthel, New types of graphene-based membranes with molecular sieve properties for He, H_2 and H_2O, J. Membr. Sci. 554 (2018) 378–384.
[17] S.J. Datta, A. Mayoral, N. Murthy Srivatsa Bettahalli, P.M. Bhatt, M. Karunakaran, I.D. Carja, D. Fan, P. Graziane, M. Mileo, R. Semino, G. Maurin, Rational design of mixed-matrix metal-organic framework membranes for molecular separations, Science 376 (2022) 1080–1087.
[18] C. Zhu, Y. Peng, W. Yang, Modification strategies for metal-organic frameworks targeting at membrane-based gas separations, Green Chem. Eng. 2 (2021) 17–26.
[19] H. Daglar, S. Aydin, S. Keskin, MOF-based MMMs breaking the upper bounds of polymers for a large variety of gas separations, Sep. Purif. Technol. 281 (2022) 119811.
[20] C. Ma, Z. Yang, X. Guo, Z. Qiao, C. Zhong, Size-reduced low-crystallinity ZIF-62 for the preparation of mixed-matrix membranes for CH_4/N_2 separation, J. Membr. Sci. 663 (2022) 121069.
[21] H.C. Gulbalkan, Z.P. Haslak, C. Altintas, A. Uzun, S. Keskin, Assessing CH_4/N_2 separation potential of MOFs, COFs, IL/MOF, MOF/Polymer, and COF/Polymer composites, Chem. Eng. J. 428 (2022) 131239.
[22] K. Chen, K. Xu, L. Xiang, X. Dong, Y. Han, C. Wang, L.-B. Sun, Y. Pan, Enhanced CO_2/CH_4 separation performance of mixed-matrix membranes through dispersion of sorption-selective MOF nanocrystals, J. Membr. Sci. 563 (2018) 360–370.
[23] C. Altintas, S. Keskin, Molecular simulations of MOF membranes and performance predictions of MOF/polymer mixed matrix membranes for CO_2/CH_4 separations, ACS Sustain. Chem. Eng. 7 (2018) 2739–2750.
[24] F. Guo, D. Li, R. Ding, J. Gao, X. Ruan, X. Jiang, G. He, W. Xiao, Constructing MOF-doped two-dimensional composite material ZIF-90@C_3N_4 mixed matrix membranes for CO_2/N_2 separation, Sep. Purif. Technol. 280 (2022) 119803.
[25] N. Habib, O. Durak, M. Zeeshan, A. Uzun, S. Keskin, A novel IL/MOF/polymer mixed matrix membrane having superior CO_2/N_2 selectivity, J. Membr. Sci. 658 (2022) 120712.
[26] Y. Yoo, V. Varela-Guerrero, H.-K. Jeong, Isoreticular metal-organic frameworks and their membranes with enhanced crack resistance and moisture stability by surfactant-assisted drying, Langmuir 27 (2011) 2652–2657.
[27] N. Hara, M. Yoshimune, H. Negishi, K. Haraya, S. Hara, T. Yamaguchi, Diffusive separation of propylene/propane with ZIF-8 membranes, J. Membr. Sci. 450 (2014) 215–223.
[28] N. Hara, M. Yoshimune, H. Negishi, K. Haraya, S. Hara, T. Yamaguchi, Metal-organic framework membranes with layered structure prepared within the porous support, RSC Adv. 3 (2013) 14233–14236.
[29] Z. Zhao, X. Ma, Z. Li, Y. Lin, Synthesis, characterization and gas transport properties of MOF-5 membranes, J. Membr. Sci. 382 (2011) 82–90.
[30] H. Daglar, S. Keskin, Combining machine learning and molecular simulations to unlock gas separation potentials of MOF membranes and MOF/polymer MMMs, ACS Appl. Mater. Interfaces 14 (2022) 32134–32148.
[31] P. Zarabadi-Poor, R. Marek, Metal-organic frameworks for helium recovery from natural gas *via* N_2/He separation: a computational screening, J. Phys. Chem. C 123 (2019) 3469–3475.
[32] Y.G. Chung, E. Haldoupis, B.J. Bucior, M. Haranczyk, S. Lee, H. Zhang, K.D. Vogiatzis, M. Milisavljevic, S. Ling, J.S. Camp, Advances, updates, and analytics for the computation-ready, experimental metal-organic framework database: CoRE MOF 2019, J. Chem. Eng. Data 64 (2019) 5985–5998.
[33] D. Ongari, P.G. Boyd, S. Barthel, M. Witman, M. Haranczyk, B. Smit, Accurate characterization of the pore volume in microporous crystalline materials, Langmuir 33 (2017) 14529–14538.
[34] A.K. Rappé, C.J. Casewit, K. Colwell, W.A. Goddard III, W.M. Skiff, UFF, a full periodic table force field for molecular mechanics and molecular dynamics simulations, J. Am. Chem. Soc. 114 (1992) 10024–10035.
[35] C.E. Wilmer, K.C. Kim, R.Q. Snurr, An extended charge equilibration method, J. Phys. Chem. Lett. 3 (2012) 2506–2511.
[36] P. Bleiziffer, K. Schaller, S. Riniker, Machine learning of partial charges derived from high-quality quantum-mechanical calculations, J. Chem. Inf. Model. 58 (2018) 579–590.
[37] X. Wang, F. Ma, S. Liu, L. Chen, S. Xiong, X. Dai, B. Tai, L. He, M. Yuan, P. Mi, Thermodynamics-kinetics-balanced metal-organic framework for in-depth radon removal under ambient conditions, J. Am. Chem. Soc. 144 (2022) 13634–13642.
[38] S.K. Singh, A.T. Sose, F. Wang, K.K. Bejagam, S.A. Deshmukh, Data driven discovery of MOFs for hydrogen gas adsorption, J. Chem. Theor. Comput. 19 (2023) 6686–6703.
[39] J.O. Hirschfelder, C.F. Curtiss, R.B. Bird, Molecular Theory of Gases and Liquids, Wiley, New York, 1954.
[40] R.B. Getman, J.H. Miller, K. Wang, R.Q. Snurr, Metal alkoxide functionalization in metal-organic frameworks for enhanced ambient-temperature hydrogen storage, J. Phys. Chem. C 115 (2011) 2066–2075.
[41] Q. Yang, D. Liu, C. Zhong, J.-R. Li, Development of computational methodologies for metal-organic frameworks and their application in gas separations, Chem. Rev. 113 (2013) 8261–8323.
[42] Z. Zhang, X. Cao, C. Geng, Y. Sun, Y. He, Z. Qiao, C. Zhong, Machine learning aided high-throughput prediction of ionic liquid@MOF composites for membrane-based CO_2 capture, J. Membr. Sci. 650 (2022) 120399.
[43] J. Nan, X. Dong, W. Wang, W. Jin, N. Xu, Step-by-step seeding procedure for preparing HKUST-1 membrane on porous α-alumina support, Langmuir 27 (2011) 4309–4312.
[44] Y. Mao, W. Cao, J. Li, Y. Liu, Y. Ying, L. Sun, X. Peng, Enhanced gas separation through well-intergrown MOF membranes: seed morphology and crystal growth effects, J. Mater. Chem. A 1 (2013) 11711–11716.
[45] M.D. Segall, P.J. Lindan, M.J. Probert, C.J. Pickard, P.J. Hasnip, S.J. Clark, M.C. Payne, First-principles simulation: ideas, illustrations and the CASTEP code, J. Phys. Condens. Matter 14 (2002) 2717.
[46] M.C. Payne, M.P. Teter, D.C. Allan, T.A. Arias, J.D. Joannopoulos, Iterative minimization techniques for *ab initio* total-energy calculations: molecular dynamics and conjugate gradients, Rev. Mod. Phys. 64 (1992) 1045.
[47] J.P. Perdew, K. Burke, M. Ernzerhof, Generalized gradient approximation made simple, Phys. Rev. Lett. 77 (1996) 3865.
[48] A. Tkatchenko, M. Scheffler, Accurate molecular van der Waals interactions from ground-state electron density and free-atom reference data, Phys. Rev. Lett. 102 (2009) 073005.
[49] Y. Sun, Z. Zhang, L. Tian, H. Huang, C. Geng, X. Guo, Z. Qiao, C. Zhong, Confined ionic liquid-built gas transfer pathways for efficient propylene/propane separation, ACS Appl. Mater. Interfaces 13 (2021) 49050–49057.
[50] X. Yuan, X. Deng, C. Cai, Z. Shi, H. Liang, S. Li, Z. Qiao, Machine learning and high-throughput computational screening of hydrophobic metal-organic frameworks for capture of formaldehyde from air, Green Energy Environ. 6 (2021) 759–770.
[51] F. Pedregosa, G. Varoquaux, A. Gramfort, V. Michel, B. Thirion, O. Grisel, M. Blondel, P. Prettenhofer, R. Weiss, V. Dubourg, Scikit-learn: machine learning in Python, J. Mach. Learn. Res. 12 (2011) 2825–2830.
[52] X. Cao, Y. He, Z. Zhang, Y. Sun, Q. Han, Y. Guo, C. Zhong, Predicting of covalent organic frameworks for membrane-based isobutene/1,3-butadiene separation: combining molecular simulation and machine learning, Chem. Res. Chin. Univ. 38 (2022) 421–427.
[53] L.C. Lin, K. Lee, L. Gagliardi, J.B. Neaton, B. Smit, Force-field development from electronic structure calculations with periodic boundary conditions: applications to gaseous adsorption and transport in metal-organic frameworks, J. Chem. Theor. Comput. 10 (2014) 1477–1488.